Mössbauer, crystal-structure, magnetic, and Raman studies of the $(Y,Ce)_2Sr_2CuFeO_8$ compound isomorphic to superconductors with the T^* structure

M. Pissas,* C. Mitros, D. Niarchos, A. Kostikas, and A. Simopoulos
Institute of Materials Science National Research Center for Physical Sciences Demokritos, 153 10 Agia Paraskevi, Attiki, Greece

M. Abrashev, V. Hadjimitov, and M. Iliev
Faculty of Physics, Sofia University, 1126 Sofia, Bulgaria
(Received 22 March 1994)

The crystal structure, the magnetic and transport properties, and the lattice vibrations of the $(Y,Ce)_2Sr_2CuFeO_8$ compound were studied by Rietveld refinement, Mössbauer spectroscopy, dc magnetic susceptibility, electrical-resistivity measurements, and Raman spectroscopy. The Rietveld-refinement results and Raman spectra show that the space group which describes the structure is $P4mm$. Mössbauer spectra can be fitted with one component with hyperfine parameters which correspond to Fe^{+3} in a high-spin state coordinated by five oxygen atoms arranged in a square pyramid. Most of the observed phonon lines can be assigned to definite atomic vibrations. Magnetic measurements show an antiferromagnetic transition at 30 K. Fitting of dc-susceptibility data in the paramagnetic region gives an effective magnetic moment of $(3.6\pm0.1)\mu_B$ per ion. The resistivity data show insulating behavior.

I. INTRODUCTION

To elucidate the nature of high-temperature superconductivity in doped layered cuprates it is interesting to study the properties on isostructural compounds, in order to establish the structural conditions that favor or inhibit the occurrence of superconductivity in these materials. It is useful to analyze the changes that take place when the copper ions are totally or partially replaced by metal ions with different coordinates and valence, and to correlate such changes with the electrical properties of these materials. Some of these compounds cannot be stabilized without the simultaneous presence of two transition elements. An example is the compound[1,2] $YBaCuFeO_5$ where the structure consists of sheets of apex-sharing oxygen pyramids whose centers are occupied by Fe or Cu. The pyramids connect by corner sharing of the equatorial oxygen ions into two-dimensional (2D) slabs that are separated by a layer of Y. The Ba ion is at the level of the apical oxygen. The Y and Ba ions occupy the dodecahedral site in the simple perovskite structure. This structure is similar to that of $YBa_2Cu_3O_{6+x}$ with the difference that the chain levels are absent.

Another compound[3] of the above category with a more complicated structure is $Y_2SrFeCuO_{6.5}$. The crystal structure has many similarities to that of $YBaCuFeO_5$. The difference is that instead of a single layer of Y^{3+} there are double layers of Y^{3+}, which are sevenfold coordinated by seven oxygen ions located at the corners of a cube with the eighth corner vacant. The Y environment is intermediate between that of the fluorite structure and that of the anion-deficient fluorite-type structure,[4] C-Y_2O_3. An interesting variation occurs by substitution of Y^{3+} by Ce^{4+}. Since CeO_2 has CaF_2 (fluorite) structure, this yields perovskites with layers which have fluorite structure. For example Michel *et al.*[5] isolated the $NdCeBaFeCuO_7$ compound which can be described as an intergrowth of $NdBaFeCuO_5$ structure and CeO_2 with fluorite structure. Wada *et al.*[6] synthesized a new homologous compound series $(Fe,Cu)Sr_2(Y,Ce)_nCu_2O_y$ which contains a multiple MO_2 unit block with fluorite structure.

Recently Kaibin *et al.*[7] prepared in single-phase form the compound $(Y,Ce)_2Sr_2CuFeO_8$. The structure of this compound is similar to the so-called T^* structure.

In this paper we report an elaborated study of the structure, lattice vibrations, magnetic, and conductivity properties of the compound $(Y,Ce)_2Sr_2CuFeO_8$ via x-ray diffraction and Mössbauer and Raman spectroscopy as well as magnetic and resistivity measurements.

II. EXPERIMENTAL DETAILS

The sample with nominal composition $Y_{1.34}Ce_{0.66}Sr_2CuFeO_8$ was prepared by thoroughly mixing high purity stoichiometric amounts of Y_2O_3, CeO_2, $SrCO_3$, CuO, and Fe_2O_3. The mixed powders were pelletized and annealed in air at 1125 °C for 24 h and after several grindings the sample was annealed at the same temperature and finally was quenched to room temperature (RT). This procedure yields a single-phase material, while any significant deviation from the above ratio of Y:Ce leads to multiphase samples.

The x-ray diffraction (XRD) patterns were taken in the Bragg-Brentano geometry (from 20° to 120° with a step of 0.03°) with Cu $K\alpha$ radiation using a graphite crystal monochromator (Siemens D500). Mössbauer spectra were taken using a conventional constant acceleration spectrometer with $^{57}Co(Rh)$ source moving at RT while the absorber was at the desired temperature. dc magnetization measurements were performed in a superconducting quantum interference device (SQUID) magnetometer

(Quantum Design).

In the Raman scattering experiments two kinds of spectra were measured. The first kind of spectra was measured using a micro-Raman triple multichannel spectrometer (Microdil 28) equipped with an optical microscope. An 100× objective lens produced a laser spot of about 1 μm in diameter and collected the scattered light from the polished surface of individual microcrystals in backward geometry. The second kind of spectra was recorded using a double spectrometer (Spex 1403) equipped with a cooled photomultiplier and photon counting system. The laser spot was between 100 and 200 μm and the scattered light characterized the pellet as a whole. Both the 488 nm and 514.5 nm Ar^+ laser lines were used for excitation.

III. RESULTS AND DISCUSSION

A. Structural study

The structure of the $(Y,Ce)_2Sr_2CuFeO_8$ compound is shown in Fig. 1. It is similar to the so-called T^* structure which consists of alternating slabs of La_2CuO_4 and Nd_2CuO_4 type structures. The layers that come from La_2CuO_4 have a structure of NaCl, while the layers that come from Nd_2CuO_4 structure have the structure of CaF_2. The connection of layers is mediated through a layer of transition element. In this way the transition metal (e.g., Cu or Fe) has approximately square pyramidal coordination.

The T^* structure, e.g., in the compound $(Nd_{0.66}Sr_{0.205}Ce_{0.135})CuO_{4-\delta}$ is described[8] by the space group $P4/nmm$ (No. 129). There is one site {M site, $2c(0,1/2,z_1)$} in which the M cation is coordinated by nine oxygen atoms as in La^{3+} in the La_2CuO_4 compound

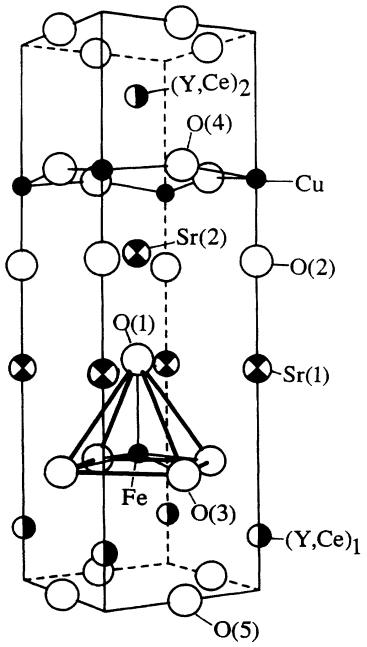

FIG. 1. Crystal structure of $(Y,Ce)_2Sr_2CuFeO_8$.

and another site {M' site, $2c(0,1/2,z_2)$} in which cation M' is coordinated by eight oxygen atoms on the corners of a cube as in Nd^{3+} in the Nd_2CuO_4 compound. The cations M and M' form double layers with the NaCl and CaF_2 structures, respectively.

The iron and copper cations in the present structure are coordinated by five oxygens arranged in a square pyramid {$2c$ site $(1/2,0,z_3)$}. Assuming that Fe and Cu occupy separate sites, we must choose a space group with lower symmetry in order to describe the structure. More specifically we choose space group $P4mm$ (No. 99). In this space group we have subtracted the diagonal glide plane so that all the $2c$ sites $(1/2,0,z)$ split into two separate sites, the $1a$ and $1b$ {$(0,0,z),(1/2,1/2,z)$}, respectively. The $4f$ site of oxygen at the (Cu,Fe) planes splits also into two $2c$ sites $(1/2,0,z)$.

Structure refinements on the $(Y,Ce)_2Sr_2CuFeO_8$ phase were carried out with the BBWS-9006 Rietveld analysis program.[9] The profile-shape functions were assumed to be Pearson VII with profile shape coefficient $m=1.1$ (Lorentzian function). The background was refined together with the structure. The refinement was carried out using the space group $P4mm$. Two different values of the isotropic thermal parameter B were assumed, one for all the cations and one for the oxygens. Occupancies of oxygen were assumed to be 1.0. All species occupying the same site were constrained to have the same atomic positions. Structural parameters, reliability factors, and the cation-oxygen bond lengths obtained from Rietveld refinement are summarized in Tables I and II. Figure 2 shows the experimental XRD spectra with that theoretically calculated, according to Rietveld refinement. As shown in Table I refinements of the cation occupancies at the M and M' sites show a clear preference of larger cations Sr^{2+} for the M site (NaCl structure). The same occurs for the Sr^{2+} in compounds $Bi_2Sr_2Ca_{n-1}Cu_nO_y$ and Sr_2FeO_4.[10] On the other hand Y and Ce occupy the M' site (CaF_2 structure). The occupancies of Y and Ce are constrained to the nominal composition of the sample. In most of the T^*-phase materials the cations are ordered with larger ones (such as La^{3+}, Nd^{3+}, and Sr^{2+}) occupying the M site while the smaller cations (such as Y^{3+}, Gd^{3+}, and Ce^{4+}) occupy the M' site.[11,8,12,13]

Because of the similarity of the scattering factors of Cu and Fe the present data cannot distinguish which site is occupied by the iron and copper ions ($1a$ or $1b$). However, by using the current literature information on Fe^{3+} and Cu^{2+}, coordinated by five oxygens arranged in a square pyramid, we can assign the distribution of iron and copper ions at the $1b$ and $1a$ positions, respectively.

The existing bond length data indicate that the copper ions are coordinated by five oxygens arranged in a square pyramid with the long Cu-O bond along the c axis. For example, in other related cuprates as in $YBa_2Cu_3O_7$ $\langle Cu\text{-}O_{eq}\rangle_{av}=1.944(1)$ Å, $Cu\text{-}O_{ax}=2.298(6)$ Å and, in $YBa_2Cu_3O_6$, $Cu\text{-}O_{eq}=1.940(0)$ Å, $Cu\text{-}O_{ax}=2.471(4)$Å.[14] For materials with T^* structure, e.g., in $La_{0.9}Cd_{0.9}Sr_{0.2}CuO_4$, $Cu\text{-}O_{eq}=1.9345(8)$ Å, $Cu\text{-}O_{ax}=2.188(1)$ Å (Ref. 11) and, in $YBaCuFeO_5$, $Cu\text{-}O_{eq}=1.936(2)$ Å, $Cu\text{-}O_{ax}=2.345(9)$Å.[15] Thus Cu^{2+}

TABLE I. Fractional atomic coordinates, isotropic temperature factors, occupancy factors, cell constants, and Rietveld-refinement reliability factors for the $(Y,Ce)_2Sr_2CuFeO_8$ sample. Rietveld refinements were done in the tetragonal space group *P4mm* (No. 99). $a=3.8239(4)$ Å, $c=12.5635(2)$ Å, $R_p=7.4$, $R_{wp}=8.2$, $R_B=5.3$. The numbers in parentheses are estimated standard deviations referred to the last significant digit.

Atom	Wyckoff notation	Site symmetry	x	y	z	B	N
Sr(1)	1*a*	$4mm(C_{4v})$	0	0	0.385(4)	0.64(5)	1.0
Sr(2)	1*b*	$4mm(C_{4v})$	1/2	1/2	0.602(4)	0.64(5)	1.0
Y(1)	1*a*	$4mm(C_{4v})$	0	0	0.095(4)	0.64(5)	0.67
Ce(1)	1*a*	$4mm(C_{4v})$	0	0	0.095(4)	0.64(5)	0.33
Y(2)	1*b*	$4mm(C_{4v})$	1/2	1/2	0.892(4)	0.64(5)	0.67
Ce(2)	1*b*	$4mm(C_{4v})$	1/2	1/2	0.892(4)	0.64(5)	0.33
Fe	1*b*	$4mm(C_{4v})$	1/2	1/2	0.253(4)	0.64(5)	1.0
Cu	1*a*	$4mm(C_{4v})$	0	0	0.752(4)	0.64(5)	1.0
O(1)	1*b*	$4mm(C_{4v})$	1/2	1/2	0.401(5)	0.83(8)	1.0
O(2)	1*a*	$4mm(C_{4v})$	0	0	0.570(5)	0.83(8)	1.0
O(3)	2*c*	$mm(C_{2v})$	1/2	0	0.237(5)	0.83(8)	1.0
O(4)	2*c*	$mm(C_{2v})$	1/2	0	0.787(5)	0.83(8)	1.0
O(5)	2*c*	$mm(C_{2v})$	1/2	0	0.0	0.83(8)	1.0

"prefers" the center of the severely elongated square pyramid.

On the other hand the FeO_5 square pyramid is somewhat squashed with an Fe-O_{ax} bond distance shorter than the Fe-O_{eq} distances. In the compound $Pb_4Fe_3O_8Cl$,[16] in which Fe^{3+} is fivefold coordinated, Fe-O_{eq}=2.01 Å and Fe-O_{ax}=1.93 Å. In the recently prepared compound $YBa_2Fe_3O_8$,[17] for the Fe at the Fe(2) site the distances are also consistent with this rule, e.g., Fe(2), $O_{eq}=2.0138(9)$ Å, Fe(2)-$O_{ax}=1.872(6)$ Å. For the compound $YBaCuFeO_5$,[1,2,15] which also has Fe^{3+} in square pyramidal coordination, Fe-$O_{ax}=1.82(9)$ Å and Fe-$O_{eq}=2.03(3)$ Å.

The results on the preference of site occupancy for Cu^{2+} and Fe^{3+} in squared pyramids support the assumption of the space group *P4mm* to refine the structural data. According to this refinement (Table I), Fe^{3+} occupies the 1*b*(1/2,1/2,0.253) and Cu^{2+} the 1*a* site (0,0,0.752). With this assignment the refinement gives the bond lengths listed in Table II i.e., Cu-$O_{eq}=1.961$ Å, Cu-$O_{ax}=2.278$ Å and Fe-$O_{eq}=1.923$ Å, Fe-$O_{ax}=1.855$ Å. A description with space group *P4/nmm* on the other hand provides one site for both iron and copper in a squashed square pyramid, (Fe,Cu)-$O_{eq}=1.94$ Å, (Fe,Cu)-$O_{ax}=1.99$ Å, which is consistent with literature data for Fe^{3+} but not for Cu^{2+}. This, together with the lower R_B value we obtain for the *P4mm* than the *P4/nmm* favors the former space group for the structure description.

TABLE II. Bond distances (Å) for $(Y,Ce)_2Sr_2CuFeO_8$ in *P4mm*.

Sr(1)-O(2)	1×2.340(3) Å
Sr(1)-O(3)	4×2.661(2) Å
Sr(1)-O(1)	4×2.712(2) Å
Sr(2)-O(1)	1×2.509(3) Å
Sr(2)-O(2)	4×.730(1) Å
Sr(2)-O(4)	4×.021(2) Å
Y(1)-O(3)	4×2.612(2) Å
Y(1)-O(5)	4×2.253(1) Å
Y(2)-O(4)	4×.324(2) Å
Y(2)-O(5)	4×.345(3) Å
Fe-O(1)	1×1.855(1) Å
Fe-O(3)	4×1.923(2) Å
Cu-O(2)	1×2.278(3) Å
Cu-O(4)	4×1.961(1) Å

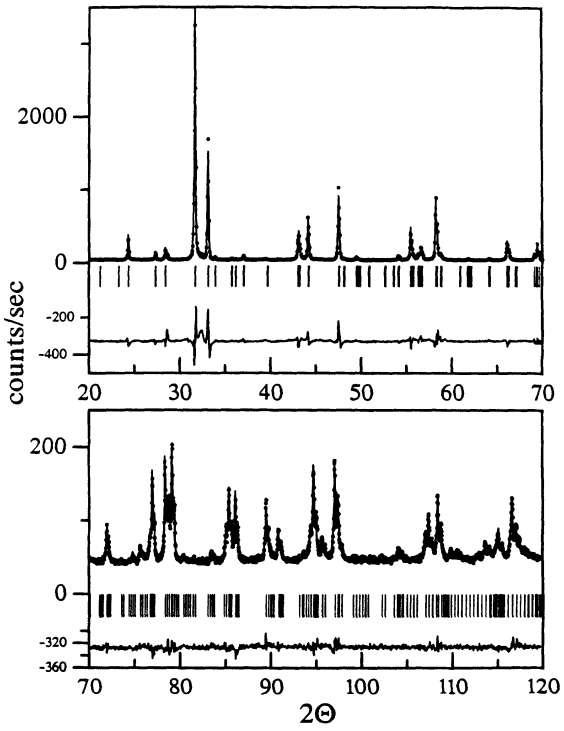

FIG. 2. Rietveld-refinement patterns for the $(Y,Ce)_2Sr_2CuFeO_8$ sample. The observed intensities are shown by dots and the calculated ones by the solid line. The positions of the Bragg reflections are shown by small vertical lines below the pattern. The line in the bottom indicates the intensity difference between the experimental and the refined pattern.

B. Raman scattering

The unit cell of $(Y,Ce)_2Sr_2CuFeO_8$ for either *P4mm* or *P4/nmm* structure contains one formula unit. It follows from Table I that for the *P4mm* structure the cations [Sr(1), Sr(2), (Y/Ce)(1), (Y/Ce)(2), Cu, and Fe], O(1), and O(2) occupy sites with C_{4v} symmetry. A nuclear-site analysis[18] shows that each of these atoms participates in two Γ-point phonon modes of A_1 and E symmetry, respectively. The remaining O(3), O(4), and O(5) atoms occupy sites of C_{2v}^v symmetry and each of them participates in four phonon modes (A_1+B_1+2E). Thus group theory predicts $10A_1+3B_1+13E$ optical phonons and two (A_1+E) acoustic phonons. The A_1 and E optical modes are both Raman and infrared active (they correspond to atomic motions along the z direction or within the xy planes, respectively). The B_1 modes are only Raman active [they correspond to motions along the z direction of the O(3), O(4), and O(5) atoms only]. The A_1 modes have to be observed in the parallel xx, yy, and zz, the B_1 in parallel xx and yy and crossed $x'y'$ (x',y' are the [110] and [1$\bar{1}$0] directions), and the E_g in crossed zx, zy, xz, and yz polarizations of the exciting and scattered light, respectively.

The phonon modes and their selection rules differ from that described above for a $M_2Sr_2M'_2O_8$ compound (M=Y or Ce, M'=Cu or Fe) characterized by the $P4/nmm(D_{4h}^7)$ space group. The M, Sr, M', and O_{Sr} [corresponding to O(1) and O(2) in the *P4mm* structure] occupy $2c$ sites of C_{4v} symmetry and each atom participates in four $(A_{1g}+A_{2u}+E_g+E_u)$ modes, and the O_M atoms [corresponding to O(5)] occupy $2a$ sites of D_{2d} symmetry and participate in four $A_{2u}+B_{1g}+E_g+E_u$ modes, whereas the $O_{M'}$ atoms [corresponding to O(3) and O(4)] are at $4f$ sites (C_{2v}^v symmetry) and participate in eight $A_{1g}+A_{2u}+B_{1g}+B_{2u}+2E_g+2E_u$ phonon modes. Of the in total 28 phonon modes $(5A_{1g}+6A_{2u}+2B_{1g}+B_{2u}+7E_g+7E_u)$ 14 are Raman active $(5A_{1g}+2B_{1g}+7E_g)$, 11 are IR active $(5A_{2u}+6E_u)$, two $(A_{2u}+E_u)$ are acoustical modes, and the B_{2u} mode is silent. The allowed scattering configurations for the A_{1g}, B_{1g}, and E_g Raman modes are the same as for the A_1, B_1, and E modes, respectively, in the *P4mm* structure.

Relying on the above considerations one expects that a comparison between the number of experimentally observed Raman lines of given symmetry with the number of Raman modes expected for *P4mm* or *P4/nmm* structures (e.g., $10A_1$ for *P4mm* or $5A_{1g}$ for *P4/nmm*) may rule out one of the possible structures. For a mixed compound such as $(Y,Ce)_2Sr_2(Cu,Fe)_2O_8$, however, the analysis may become ambiguous as the existence of different atoms at equivalent sites may result in two-mode behavior of the phonons belonging to phonon branches that change significantly with elemental substitution. The effect of substitution may be considered as lowering the local symmetry. The vibrational frequencies and their selection rules for the mixed $(Y,Ce)_2Sr_2(Cu,Fe)_2O_8$ system (*P4/nmm*) may become then similar to those of Cu-Fe-ordered $(Y,Ce)_2Sr_2CuFeO_8$ (*P4mm*) compound.

Typical Raman spectra of $(Y,Ce)_2Sr_2CuFeO_8$ with zz and xx polarization geometries as obtained from zx-oriented microcrystal surfaces are shown in Fig. 3. The high-frequency doublet with components at 644 cm^{-1} and 627 cm^{-1} is of higher intensity in the zz spectra, and the strong peak at 475 cm^{-1} is zz polarized, whereas the one at 445 cm^{-1} is xx polarized. Although present in both types of spectra, the low-frequency peaks at 152 cm^{-1}, 176 cm^{-1}, and 320 cm^{-1} are better pronounced with the xx polarization. The spectral features in the crossed zx spectra were extremely weak and thus the E_g phonons allowed for this geometry will not be discussed.

The Raman scattering of $(Y,Ce)_2Sr_2CuFeO_8$ will be discussed further assuming the more relevant *P4mm* structure and in close comparison with the existing data for the Raman and IR phonons and the lattice dynamical calculations of the simpler analog of this, the compound[19] $YBaCuFeO_5$. Both structures contain Cu-O and Fe-O planes; however, $(Y,Ce)_2Sr_2CuFeO_8$ contains $(Y,Ce)_2$-O_2 fluorite-type slabs instead of single Y layers and Sr_2-O_2 "rocksalt"-type slabs instead single of Ba-O layers.

In the low-frequency region (below 250 cm^{-1}) the A_1 phonons originating from the heavier atoms Sr, Cu, Fe, and Y/Ce should occur. The polarized measurements on a xy-oriented surface (the results are not given in Fig. 3), allowing to separate the A_1 and B_1 lines, showed that the 152 cm^{-1} and 176 cm^{-1} lines were of predominantly B_1 symmetry. As the latter lines were observed also in the zz spectra a conclusion could be drawn that they are of mixed A_1+B_1 symmetry. In the B_1 modes the motions involved are only of the O(3), O(4), and O(5) atoms (the oxygens from the Fe, Cu, and Y/Ce layers, respectively). In the layered cuprates, e.g., the Y-, Bi-, or Tl-based T^* systems, characterized by a single B_{1g} (or pseudo-B_{1g}) mode originating from the out-of-phase motions of the oxygen atoms of the Cu-O planes (or from the Nd fluorite

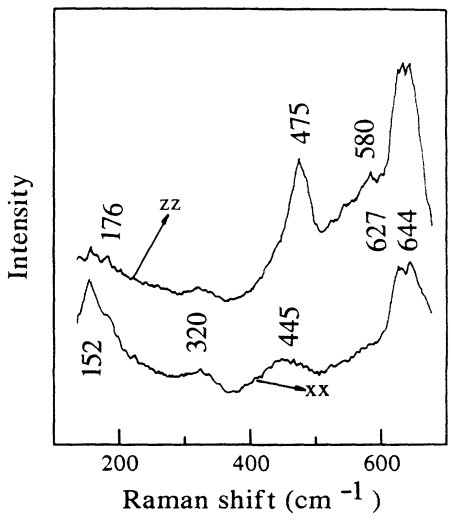

FIG. 3. zz- and xx-polarized Raman spectra of $(Y,Ce)_2Sr_2CuFeO_8$ as obtained in a backward scattering geometry from a zz-oriented microcrystal surface (λ_L=488.0 nm). The two spectra are shifted for clarity.

slabs as is for Nd_2CuO_4), the B_{1g} frequency is about[20,21] 320 ± 30 cm^{-1}. The coexistence of inequivalent Cu-O and Fe-O planes in the *P4mm* structure results in two B_1 modes corresponding to the "odd" and "even" vibrations of the oxygen atoms of these planes (they correspond to the B_{2u} and B_{1g} modes in the higher-symmetry space group *P4/nmm*). For $YBaCuFeO_5$ the two B_1 phonons were found[19] at 180 and 345 cm^{-1}. In a similar manner we assign the 152 and 320 cm^{-1} lines B_1 modes corresponding, respectively, to the O(3)-O(4)-O(5) in-phase and O(3)-O(4) in-phase O(5) out-of-phase motions. The 152 cm^{-1} line is additionally overlapped by the A_1 modes of some cations.

The high-frequency doublet at 627 and 644 cm^{-1} can tentatively be assigned to either the A_1 phonon of O(1) (Fe apex oxygen), exhibiting two-mode behavior due to the Ce for Y substitution, or to the two A_1 phonons of O(1) and O(2) (Cu apex oxygen). We note here that the apex oxygen A_1 frequency in studies of other compounds with Fe-based pyramids so far is also high: 691 cm^{-1} for $YBa_2Fe_3O_8$ (Ref. 22) and 669 cm^{-1} for $YBaCuFeO_5$.[19] Also the peak at 580 cm^{-1} can be assigned tentatively to either the A_1 mode of O(2) or to a disorder-induced Raman scattering of phonon density-of-states origin.

We assign the two phonons at 445 cm^{-1} and 475 cm^{-1} to the A_1 modes of in-phase vibrations along the *c* axis of the O(4) (from the Cu planes) and O(3) (from the Fe planes) atoms. The former frequency is the typical one for this mode in the layered nonsuperconducting cuprates (e.g., the oxygen-deficient $YBa_2Cu_3O_{6+\delta}$) where it is also *xx* polarized.[23] An analog of the 475 cm^{-1} mode has recently been observed in $YBa_2Fe_3O_8$ at 480 cm^{-1} with the same *zz* polarization.[22] Interestingly, in $YBaCuFeO_5$ instead of these two modes one observes[19] a single mode at an intermediate frequency of 456 cm^{-1}.

Figure 4 shows the nonpolarized macro-Raman spectrum of $(Y,Ce)_2Sr_2CuFeO_8$ in a wide spectral range. The dominating feature is a broadband centered at about 2000 cm^{-1} with a bandwidth $\Gamma\approx1500$ cm^{-1}. Similar broad Raman bands have been observed for many nonsuperconducting antiferromagnetic layered cuprates and have been assigned to two-magnon Raman scattering. In the one-phonon part of the spectrum only the strong 640 cm^{-1} doublet, discussed above, can be distinguished. At 1330 and 1590 cm^{-1} one observes two clearly pronounced relatively narrow lines. In the case of $YBa_2Cu_3O_6$ a single peak at 1250 cm^{-1} has also been observed, its phononic origin has been identified by isotopic replacement of the oxygen, and second-order phonon processes have been discussed.[24] Obviously, the observed two high-frequency lines in our case can also be assigned to two-phonon Raman scattering (at the Brillouin zone boundary) involving phonon branches related to the two types of apex oxygen.

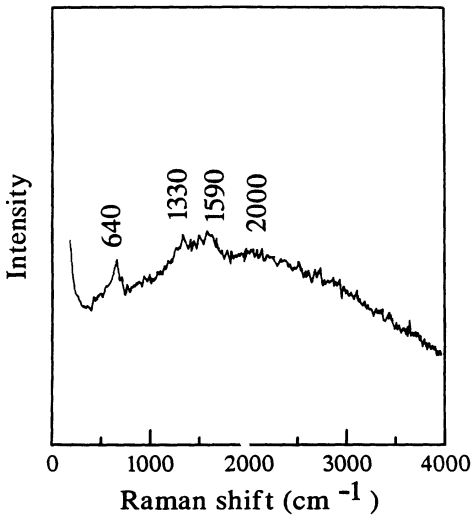

FIG. 4. Nonpolarized macro-Raman spectrum of $(Y,Ce)_2Sr_2CuFeO_8$ ceramics ($\lambda_L=488.0$ nm).

C. Magnetization and resistance measurements

Figure 5(a) shows the temperature dependence of the magnetic susceptibility (χ) of the $(Y,Ce)_2Sr_2CuFeO_8$ compound in an applied field of 1 kG. The zero field

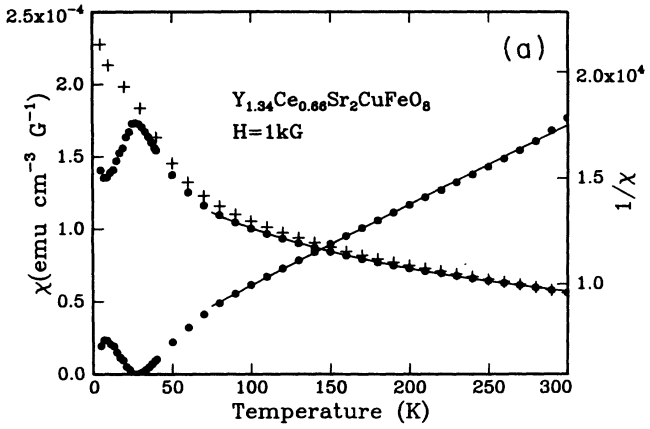

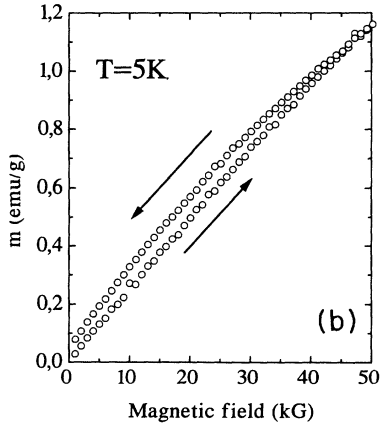

FIG. 5. (a) Magnetic susceptibility χ in zero field cooled (●) and in field cooled (+) vs temperature for sample $(Y,Ce)_2Sr_2CuFeO_8$ in a field of 1 kG. The solid line for $T\geq100$ K represents a least-squares fit of the Curie-Weiss law. The $1/\chi$ vs temperature plot for zero field cooled data is shown. (b) Magnetization vs magnetic field at 5 K.

cooling $\chi^{ZFC}(T)$ exhibits a cusplike maximum centered around 30 K. The field cooling $\chi^{FC}(T)$ is similar to the $\chi^{ZFC}(T)$ data for $T>30$ K, while for $T<30$ K $\chi^{FC}(T)$ increases when the temperature decreases down to 5 K. Figure 5(b) shows the isothermal magnetization versus applied field at 5 K for fields up to 50 kG. The virgin curve is linear up to 30 kG where a tiny hysteresis loop is opened when the field is decreased. At the low-field region the virgin curve is parallel with the "decreasing field" curve which indicates that a constant magnetic moment is created for $H \geq 30$ kG. Hysteresis between $\chi^{FC}(T)$ and $\chi^{ZFC}(T)$ can be attributed to spin glass (SG) behavior. However, $\chi^{FC}(T)$ does not attain the characteristic plateau below T_f, generally seen in SG's such as the metallic[25] $Cu_{1-x}Mn_x$ and the insulating[26] $Fe_{0.5}Mn_{0.5}TiO_3$. The zero-field measurements and the linear M versus H curve at 5 K strongly support an antiferromagnetic ordering. The difference between $\chi^{ZFC}(5)$ and $\chi^{FC}(5)$ is comparable to the magnitude of the remanent magnetization. This fact may imply that both in the field cooling processes from above $T=30$ K and in 3 T at 5 K, the external field causes the spins to cant slightly out of their original directions. Similar behavior has been recently reported[27] for the $YBa_2Fe_3O_8$ compound. If we accept the peak of $\chi^{ZFC}(T)$ at 30 K to an antiferromagnetic transition with $T_N=30$ K, this is quite low with respect to the $YBaCuFeO_5$ and $Y_2SrFeCuO_{6.5}$ compounds where T_N is 442 K and 265 K, respectively. In isomorphic compound[28] $La_{1.8}Tb_{0.2}CuO_{4+y}$, T_N suddenly decreases after doping with Sr or after an increase of y. Similarly the low T_N in the $(Y,Ce)_2Sr_2CuFeO_8$ compound can be attributed to the doping, because if we consider that Ce is in the Ce^{4+} form, there is a lack of 0.34 electrons per formula unit.

For $T \geq 100$ K the susceptibility χ can be described with the Curie-Weiss law $\chi=C/(T-\Theta)+\chi_0$ where C is given by the relation

$$C=\frac{\mu_{\text{eff}}^2 N}{3k_B}, \tag{1}$$

where N is the number of magnetic ions per unit volume, μ_{eff} is the effective magnetic moment, and k_B is the Boltzmann constant. Fitting the susceptibility data for $H=1$ kG and $100\ \text{K} \leq T \leq 300$ K gives $\mu_{\text{eff}} \simeq (3.6 \pm 0.1)\mu_B$. Assuming that for Fe^{3+} $L=0$, $S=5/2$ $S=5/2$ hold and for Cu^{2+} $L=0$, $S=1/2$ hold, the theoretical μ_{eff} for a mixture 50% iron and 50% copper is $4.35\mu_B$. The fitted value of Θ was found $\Theta \approx -187 \pm 10$ K. The negative sign of Θ indicates antiferromagnetic interactions between the magnetic moments. A molecular field approximation for a two-sublattice system predicts that $T_N=-\Theta$. This relation does not hold in our case. In a generalized molecular field theory Θ is determined by the strength and magnitude of the exchange interactions and can be written[29]

$$\Theta=\frac{2S(S+1)}{3k_B}\sum_{m=1}^{N} z_m J_m, \tag{2}$$

where z_m is the number of mth nearest neighbors of a given atom, J_m is the exchange interaction between mth neighbors, and N is the number of sets of neighbors for which $J_m \neq 0$. The quantity Θ is just the algebraic sum of all the exchange interactions on a given ion. The value of $\Theta \simeq -187$ K points out the existence of strong local antiferromagnetic interactions over T_N.

Figure 6 displays the variation of the resistance as a function of temperature for the $(Y,Ce)_2Sr_2CuFeO_8$ compound. The resistance indicates insulating behavior. The resistance increases with decreasing temperature at a much faster rate for temperatures below 70 K than above. In the inset of Fig. 6 the $\ln(R)$ vs $1/T^{1/4}$ plot of the data is presented which shows linear behavior. Therefore the resistance follows the relation $R \propto \exp[(T^*/T)^{1/4}]$ which is characteristic of an insulator where conduction can take place by uncorrelated variable range hopping processes.[30]

D. Mössbauer spectra

In Fig. 7 the ^{57}Fe Mössbauer spectra of $(Y,Ce)_2Sr_2CuFeO_8$ at RT and at 4.2 K are presented. The parameters obtained from the least-squares fit are listed in Table III. At RT the spectrum can be fitted by one quadrupole doublet with isomer shift $\delta=0.262$ mm/s with respect to α-Fe at RT and quadrupole splitting $\Delta=0.432$ mm/s. At 4.2 K the spectrum displays magnetic hyperfine structure which can be fitted with one magnetic sextet component with hyperfine parameters $\delta=0.386$ mm/s, $\varepsilon=-0.087$ mm/s, $H=490$ kG, and $\Delta H=10$ kG. We must note that the Mössbauer spectra at 85 K contain both a magnetically split sextet and a paramagnetic doublet which is similar to that obtained at RT. This behavior is anomalous because the magnetic susceptibility shows a transition at 30 K, while Mössbauer spectroscopy continues to detect a fairly large internal field well above 30 K. This behavior is not unusual as for example at the $Nd_{2-x}Ce_xCuO_{4+y}$ compound Mössbauer spectroscopy[31] detects a large internal field well above T_N which was explained assuming the ex-

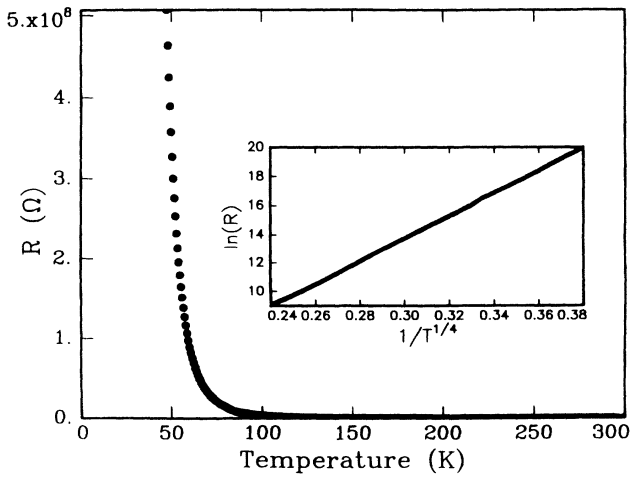

FIG. 6. Resistance vs temperature for the $(Y,Ce)_2Sr_2CuFeO_8$ compound from 30 K to RT. The inset shows the resistivity in logarithmic scale vs $T^{-1/4}$.

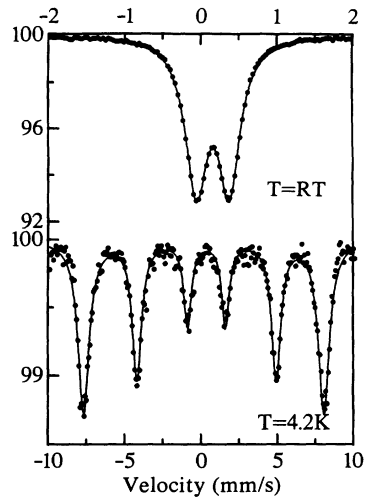

FIG. 7. Mössbauer spectra of $(Y,Ce)_2Sr_2CuFeO_8$ (a) RT, (b) 4.2 K. The ordinate axis is relative transmission.

istence of spin clusters of variable size. The spin clusters are formed due to extremely long-lived ($>10^{-8}$ s) 2D spin correlations far above the 3D Néel temperature. It is generally accepted that for a given oxidation state and for identical ligands a decrease of the iron coordination number leads to a decrease of the isomer shift.[32] For example the value of the isomer shift for Fe^{3+} in square pyramidal coordination is smaller than the isomer shift of Fe^{3+} in octahedral coordination at the same temperature. The isomer shift of iron in $ReBaCuFeO_5$, coordinated by a square pyramid ($\delta=0.30$ mm/s at RT and $\delta=0.39$ mm/s at 4.2 K),[2] is close to our values for $(Y,Ce)_2Sr_2CuFeO_8$. Similarly, for $La_2MCu_2O_6$ (M=Sr, Ca) which contains a site with a square pyramid arrangement the reported isomer shifts vary from 0.22 mm/s up to 0.28 mm/s.[33–35] The isomer shifts of the Fe^{3+} ion in the squared pyramidal arrangement [Cu(2) site] in the compound $YSr_2Cu_2FeO_7$ (Ref. 36) are $\delta=0.265$ mm/s at RT and 0.378 mm/s at 4.2 K. In the $Bi_{2-x}Pb_xSr_2Bi_{n-1}Fe_nO_y$ compounds[37] where the Fe^{3+} is coordinated with an octahedron of oxygen the isomer shift at RT is $\delta=0.35$ mm/s. From the value of the isomer shift and of the hyperfine magnetic field at 4.2 K we can conclude that the iron ion is in a high-spin Fe^{3+} state coordinated by five oxygen ions arranged in a square pyramid.

Since the Fe^{3+} ion can occupy 1b or 1a sites in the $(Y,Ce)_2Sr_2CuFeO_8$ compound with site symmetry 4mm (C_{4v}), the electric field gradient (EFG) tensor in the crystallographic axis will be axially symmetric ($V_{ij}=0$ for $i\neq j$) and $\eta=(V_{xx}-V_{yy})/V_{zz}=0$. Then the quadrupole splitting Δ is given by the relation

$$\Delta=(1/2)e^2|q|Q \tag{3}$$

in the paramagnetic region and

$$\Delta=(1/4)e^2|q|Q(3\cos^2\theta-1) \tag{4}$$

in the magnetic region, where θ is the angle between the z principal axis of the EFG tensor (which coincides with the c axis) and the hyperfine magnetic field, e is the electron charge, and q is equal to electric field gradient along the z axis. From the value of Δ at RT and 4.2 K using the relations (3) and (4), we find $\theta\cong 75°$ if $q>0$ and $\theta\cong 39°$ if $q<0$.

According to the results from the discussion of the structure and Raman spectra, the structure can be described from space group $P4mm$. In this description there exist two sites for Fe and Cu to occupy. We can make the following assumptions for the site occupancies: (a) The majority of Fe^{3+} occupies site 1b ($z=0.253$) and the minority site 1a ($z=0.752$), (b) equal occupation of sites 1a and 1b by Fe^{3+} and Cu^{2+} ions. The estimation of Δ using the point charge approximation gives the following quadrupole splitting values for the two cases: (a) $\Delta(1a)=1.47$ mm/s, $\Delta(1b)=0.84$ mm/s, (b) $\Delta(1a)=1.22$ mm/s, $\Delta(1b)=1.10$ mm/s. Since the Mössbauer spectrum consists of a single doublet with a quadrupole splitting of $\Delta=0.43$ mm/s, the above calculations indicate that the first case (a) gives quadrupole splitting for the 1b site close to experimental. The latter possibility (b) and any distribution of Fe in two sites can be excluded since the expected difference in the quadrupole splitting and in the isomer shift between the two sites would lead to line broadening in the Mössbauer spectra which is not observed experimentally.

TABLE III. Experimental values of the half linewidth $\Gamma/2$ in mm/s, the isomer shift δ relative to metallic Fe at RT in mm/s, the quadrupole shift ε in mm/s $\varepsilon=(1/4)e^2qQ(1+\eta^2/3)^{1/2}$, $\varepsilon=(1/8)e^2qQ(3\cos^2\theta-1+\eta\sin^2\theta\cos2\phi)$ for paramagnetic and magnetic spectra, respectively, the hyperfine magnetic field H in kG, and the hyperfine magnetic field spread ΔH modulating the linewidths, as obtained from least-squares fits of the Mössbauer spectra. The numbers in parentheses are estimated standard deviations referred to the last significant digit.

T	$\Gamma/2$	δ	ε	H	ΔH
RT	0.1692(2)	0.262(1)	0.2160(2)	0	0
5 K	0.270(0)	0.386(4)	−0.087(4)	490	10

IV. CONCLUSIONS

We have prepared and characterized the $(Y,Ce)_2Sr_2CuFeO_8$ compound. The Rietveld-refinement and Raman results indicate that the space group which describes the structure is $P4mm$. Mössbauer spectra can be fitted with one component with hyperfine parameters which correspond to Fe^{+3} in a high-spin state coordinated by five oxygens arranged in a square pyramid. These data in conjunction with the Rietveld-refinement and Raman results point to the occupation of distinct layers by Cu and Fe ions. Magnetic measurements show an antiferromagnetic transition at 30 K. Fitting in the paramagnetic region of dc susceptibility gives an effective magnetic moment of $(3.6\pm0.1)\mu_B$. The resistivity data show that the $(Y,Ce)_2Sr_2CuFeO_8$ compound is an insulator where conduction takes place by an uncorrelated variable range hopping process.

ACKNOWLEDGMENTS

Partial support for this work was provided by the E.C. through the B/E-CT91-472 project, 89EK19 of the Greek Ministry of Industry and Technology, and Grant No. F1/91 of the Bulgarian National Foundation for Science. We wish to acknowledge V. Vlesides for magnetic measurements and for his expert technical support. We would like also to thank Dr. E. Delvin for stimulating discussions.

*Electronic address: pissas@cyclades.nrcps.ariadne-t.gr

[1]L. Er-Rakho, C. Michel, P. Lacorre, and B. Raveau, J. Solid State Chem. **73**, 531 (1988).

[2]M. Pissas, C. Mitros, G. Kallias, V. Psycharis, A. Simopoulos, A. Kostikas, and D. Niarchos, Physica C **192**, 35 (1992).

[3]J. S. Kim, J. Y. Lee, J. S. Swinnea, H. Steinfink, W. M. Reiff, P. Lightfoot, S. Pei, and J. D. Jorgensen, J. Solid State Chem. **90**, 331 (1991).

[4]B. G. Hyde and S. Andersson, *Inorganic Crystal Structures* (John Wiley & Sons, New York, 1989), p. 194.

[5]C. Michel, M. Hervieu, and B. Raveau, J. Solid State Chem.

[6]T. Wada, A. Nare, A. Incinose, H. Yamauchi, and S. Tanaka, Physica C **192**, 181 (1992).

[7]T. Kaibin, Q. Yitai, L. Rukang, C. Zuyao, L. Bin, and J. Yunbo, Physica C **205**, 406 (1993).

[8]H. Sawa, S. Suzuki, M. Watanabe, J. Akimitsu, H. Matsubara, H. Watabe, S. Uchida, K. Kokusho, H. Asano, F. Izumi, and E. Takayama-Muromachi, Nature **337**, 347 (1989).

[9]D. B. Wiles and R. A. Young, J. Appl. Crystallogr. **14**, 149 (1981).

[10]S. E. Dann, M. T. Weller, and D. B. Currie, J. Solid State Chem. **92**, 237 (1991).

[11]G. H. Kwei, R. B. VonDreele, S. W. Cheong, Z. Fisk, and J. D. Thompson, Phys. Rev. B **41**, 1889 (1990).

[12]Y. Tokura, H. Takagi, and S. Uchida, Nature **337**, 345 (1989).

[13]F. Izumi, E. Takayama-Muromachi, A. Fujimori, T. Kamiyama, H. Asano, J. Akimitsu, and H. Sawa, Physica C **158**, 440 (1989).

[14]J. D. Jorgensen, B. W. Veal, A. P. Paulikas, L. J. Nowicki, G. W. Grabtree, H. Claus, and W. K. Kwok, Phys. Rev. B **41**, 1863 (1990).

[15]A. W. Mombru, C. Christides, A. Lappas, K. Prassides, M. Pissas, C. Mitros, and D. Niarchos, Inorg. Chem. **33**, 1255 (1994).

[16]J. Pannetier and P. Batall, J. Solid State Chem. **39**, 15 (1981).

[17]Q. Huang, P. Karen, V. L. Karen, A. Kjekshus, J. W. Lynn, A. D. Mighell, N. Rosov, and A. Santoro, Phys. Rev. B **45**, 9611 (1992).

[18]D. L. Rousseau, R. P. Bauman, and S. P. S. Porto, J. Raman Spectrosc. **10**, 253 (1981).

[19]Y. K. Atanassova, V. N. Popov, G. G. Bogachev, M. N. Iliev, C. Mitros, V. Psycharis, and M. Pissas, Phys. Rev. B **47**, 15201 (1993).

[20]G. Thomsen, in *Light Scattering in Solids VI,* edited by M. Cardona and G. Güntherodt, Topics of Applied Physics Vol. 68 (Springer, Berlin, 1991), p. 285.

[21]V. G. Hadjiev, I. Z. Kostadinov, L. Bozukov, E. Dinolova, and D. M. Mateev, Solid State Commun. **71**, 1093 (1989).

[22]Y. K. Atanassova, V. G. Hadjiev, P. Karen, and A. Kjekshus, Phys. Rev. B **50**, 586 (1994).

[23]M. N. Iliev and V. G. Hadjiev, J. Phys. Condens. Matter **2**, 3135 (1990).

[24]C. Thomsen, E. Schönherr, B. Friedl, and M. Cardona, Phys. Rev. B **42**, 943 (1990).

[25]S. Nagata, P. H. Keesom, and H. R. Harrison, Phys. Rev. B **19**, 1633 (1979).

[26]A. Ito, H. Aruga, E. Torikai, M. Kikuchi, Y. Syono, and H. Takei, Phys. Rev. Lett. **57**, 483 (1986).

[27]I. Felner, I. Nowik, U. Yaron, O. Cohen, E. R. Bauminger, T. Kroener, and G. Czjzek, Phys. Rev. B **48**, 16040 (1993).

[28]A. Lappas, Ph.D. thesis, University of Sussex, 1993.

[29]J. Smart, *Effective Field Theories of Magnetism* (W. B. Saunders Company, Philadelphia, London, 1966), p. 66.

[30]N. F. Mott and E. A. Davis, *Electronic Processes in Non-Crystalline Materials,* 2nd ed. (Oxford University Press, London, 1979).

[31]V. Chechersky, N. S. Kopelev, Beom-hoam O, M. I. Larkin, J. L. Peng, J. T. Market, R. L. Greene, and A. Nath, Phys. Rev. Lett. **70**, 3355 (1993).

[32]F. Menil, J. Phys. Chem. Solids **46**, 763 (1985).

[33]I. Felner, D. Hechel, E. R. Yacoby, G. Hilscher, T. Holubar, and G. Schaudy, Phys. Rev. B **47**, 12190 (1993).

[34]T. Furubayashi, K. Kinoshita, T. Yamada, and T. Matsumoto, Physica C **204**, 315 (1993).

[35]C. Meyer, F. Hartmann-Boutron, Y. Gros, and P. Strobel, Physica C **181**, 1 (1991).

[36]M. Pissas, G. Kallias, A. Simopoulos, A. Kostikas, and D. Niarchos, Phys. Rev. B **46**, 14119 (1992).

[37]M. Pissas, A. Simopoulos, A. Kostikas, and D. Niarchos, Physica C **176**, 227 (1991).